Slater to Mott Crossover in the Metal to Insulator Transition of $Nd_2Ir_2O_7$

M. Nakayama,[1] Takeshi Kondo,[1,*] Z. Tian,[1] J. J. Ishikawa,[1] M. Halim,[1] C. Bareille,[1] W. Malaeb,[1,2] K. Kuroda,[1] T. Tomita,[1] S. Ideta,[3] K. Tanaka,[3] M. Matsunami,[4] S. Kimura,[5] N. Inami,[6] K. Ono,[6] H. Kumigashira,[6] L. Balents,[7] S. Nakatsuji,[1,8] and S. Shin[1]

[1]*ISSP, University of Tokyo, Kashiwa, Chiba 277-8581, Japan*
[2]*Physics Department, Faculty of Science, Beirut Arab University, Beirut 11-5020, Lebanon*
[3]*UVSOR Facility, Institute for Molecular Science, Okazaki 444-8585, Japan*
[4]*Toyota Technological Institute, Nagoya 468-8511, Japan*
[5]*Graduate School of Frontier Biosciences, Osaka University, Suita, Osaka 565-0871, Japan*
[6]*Institute of Materials Structure Science, High Energy Accelerator Research Organization (KEK), Tsukuba, Ibaraki 305-0801, Japan*
[7]*Kavli Institute for Theoretical Physics, Santa Barbara, California 93106, USA*
[8]*CREST, Japan Science and Technology Agency (JST), 4-1-8 Honcho Kawaguchi, Saitama 332-0012, Japan*

(Received 18 March 2016; published 27 July 2016)

We present an angle-resolved photoemission study of the electronic structure of the three-dimensional pyrochlore iridate $Nd_2Ir_2O_7$ through its magnetic metal-insulator transition. Our data reveal that metallic $Nd_2Ir_2O_7$ has a quadratic band, touching the Fermi level at the Γ point, similar to that of $Pr_2Ir_2O_7$. The Fermi node state is, therefore, a common feature of the metallic phase of the pyrochlore iridates. Upon cooling below the transition temperature, this compound exhibits a gap opening with an energy shift of quasiparticle peaks like a band gap insulator. The quasiparticle peaks are strongly suppressed, however, with further decrease of temperature, and eventually vanish at the lowest temperature, leaving a nondispersive flat band lacking long-lived electrons. We thereby identify a remarkable crossover from Slater to Mott insulators with decreasing temperature. These observations explain the puzzling absence of Weyl points in this material, despite its proximity to the zero temperature metal-insulator transition.

DOI: 10.1103/PhysRevLett.117.056403

The 5*d* iridium oxides (iridates), having comparable scales for their kinetic energy, Coulomb interaction, and spin-orbit coupling, provide an excellent platform for studying new types of strongly correlated phenomena [1–11]. Amongst them, the pyrochlore iridates ($Ln_2Ir_2O_7$, where Ln is a lanthanide), endowed with frustrated geometry and cubic symmetry, have a particularly fascinating phase diagram. $Pr_2Ir_2O_7$, with the largest Ln ion, is a metallic spin liquid [12–14] and exhibits an anomalous Hall effect [15,16]. For Ln ions with a smaller ionic radius, an antiferromagnetically ordered insulating phase appears at low temperature.

Theoretically, topological band structures have been ascribed to the $Ln_2Ir_2O_7$ series [4,7,17–19]. The metallic phase is predicted to exhibit quadratically, dispersing conduction and valence bands touching at the Γ point close to the Fermi level (E_F) [20,21]. This structure has been recently identified by angle-resolved photoemission spectroscopy (ARPES) in $Pr_2Ir_2O_7$ [22]. Theory predicts that such a quadratic Fermi node state may be converted into various topological states such as a topological insulator or a Weyl semimetal by appropriate symmetry breaking [4,7,17–19].

Antiferromagnetism in these materials is of the Ising type, consisting of an "all-in–all-out" (AIAO) configuration of Ir moments on alternating tetrahedra [23–26]. This can be considered an "octupolar" spin order which breaks time-reversal but preserves cubic symmetry, and does not enlarge the unit cell [27]. The Ising nature implies two types of domains, which have recently been shown, in agreement with theoretical predictions [28], to be separated by metallic domain walls [29,30], which have been imaged by microwave impedance microscopy in the magnetic state of $Nd_2Ir_2O_7$ [26]. Early density functional studies predicted the magnetic state to be a Weyl semimetal [7], and general arguments imply that, if a quasiparticle picture applies at low energy in the antiferromagnetic phase, and the magnetic ordering is weak, it must exhibit Weyl points and cannot have a true gap. Nevertheless, optical [31] and transport [29] measurements indicate a gapped insulating ground state for $Nd_2Ir_2O_7$, despite its low antiferromagnetic–metal-insulator (MI) transition temperature $T_{MI} \approx 30$ K and proximity to metallic $Pr_2Ir_2O_7$. This begs the question of whether the weakness of the order, the quasiparticle assumption, or both, break down in this system. More generally, we seek to understand the influence of the MI transition on the conduction electrons.

In this Letter, we use ARPES to investigate the evolution of the electronic structure through the MI transition in $Nd_2Ir_2O_7$, which is the most suitable member of the series for such study because its low T_{MI} minimizes thermal broadening. Although the layered iridates have been extensively studied by photoemission [2,32–38], ours is

the first study across a MI transition in any iridate, since the latter occurs only in the pyrochlores. Using high-quality single crystals, we are able to directly measure both the single particle excitations of the metallic and insulating phases. Our data indicate that $Nd_2Ir_2O_7$ displays a dramatic Slater to Mott crossover with reducing temperature. This implies that Weyl fermions, if they exist, may do so only in a narrow region of temperature slightly below T_{MI}, in which the order is, indeed, weak and quasiparticles can survive.

Single crystals of $Nd_2Ir_2O_7$ with ~ 1 mm^3 size were grown with a flux method. The surface measured by ARPES is the (111) plane. To get a clean surface, a typical cleavage method was used: a top post glued on the crystal surface is hit *in situ* to break the crystal. Flat, shiny portions exposed on the cleaved surface are tiny, but still large enough to be illuminated by the synchrotron beam (~ 100 μm in spot size). The ARPES experiments were performed at BL7U of the UVSOR facility with a MBS A-1 analyzer ($h\nu = 8$–18 eV) [39], BL28A of Photon Factory in KEK with a Scienta SES2002 analyzer ($h\nu = 39$–60 eV), and 1^3 beam line in BESSY-II at Helmholtz-Zentrum Berlin with a Scienta R4000 analyzer ($h\nu = 50$–60 eV). The overall energy resolution in ARPES was set to ~ 15 meV, and the lowest achievable temperature was 1 K.

As previously reported, the transition temperature T_{MI} in $Ln_2Ir_2O_7$ [40] is controlled by the Ln ion size [41], the pressure [41,42], and the off stoichiometry [43]. We have selected three pieces of $Nd_2Ir_2O_7$ crystals with different transition temperatures to investigate the variation of the MI transition with small changes in stoichiometry [29,43,44]. We identified, with an electron-probe micro-analysis (EPMA), a slight deviation from stoichiometry in the Ir/Nd ratio of approximately 1% and 2% for the single crystals with zero field T_{MI} of ~ 25 K and ~ 20 K, respectively. The off stoichiometry of the crystals with the maximum T_{MI} of ~ 35 K is below the threshold of detecting in EPMA, i.e., no larger than that in the $T_{MI} \sim 25$ K samples.

Figure 1 shows the resistivity, $\rho(T)$, of the crystals we used for ARPES; note that we retrieved the crystal-piece after the ARPES experiment and measured the resistivity of exactly the same piece to properly compare the ARPES and resistivity results. The temperature derivative of $\rho(T)$, $d\rho(T)/dT$, (inset panel) enables us to estimate the value of T_{MI} from the onset of its reduction. As marked by arrows, different transition temperatures T_{MI} of ~ 19 K, ~ 25 K, and ~ 36 K were estimated for the three samples, which are, thus, labeled as MI19K, MI25K, and MI36K for the rest of the Letter.

In Fig. 2, we examine the band structure in the metallic phase. Figure 2(c1) plots the typical ARPES spectra energy distribution curves (EDCs) obtained at $(k_x, k_y) = (0, 0)$ with low-energy photons (9.0 eV $\leq h\nu \leq 11.5$ eV) corresponding to k_z (or $k_{(111)}$) values in the first Brillouin zone (BZ). Small but sharp quasiparticle peaks are observed for all of the photon energies as marked by arrows in Fig. 2(c1).

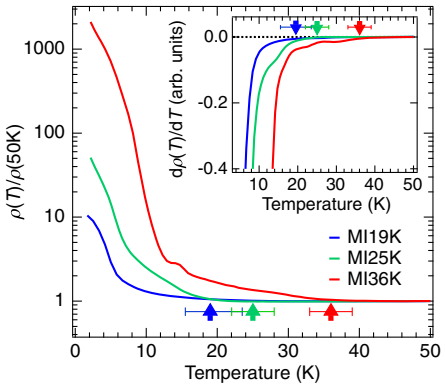

FIG. 1. Temperature dependence of the resistivity, $\rho(T)$, for $Nd_2Ir_2O_7$ crystals (MI19K, MI25K, and MI36K) we used for ARPES measurements. It is normalized to the intensity at $T = 50$ K. Inset panel plots the temperature derivative of the resistivity, $d\rho(T)/dT$. The transition temperature (T_{MI}) estimated is marked by an arrow.

We find that the quasiparticle peak approaches E_F with increasing photon energies and moves away again after getting closest to it at $h\nu = 10.5$ eV. In Fig. 2(c2), the EDCs are symmetrized about E_F to remove the effect of the Fermi cutoff [22,45]. We found that the gapped spectra with two peaks merge to one peak at 10.5 eV; thus, the band touching

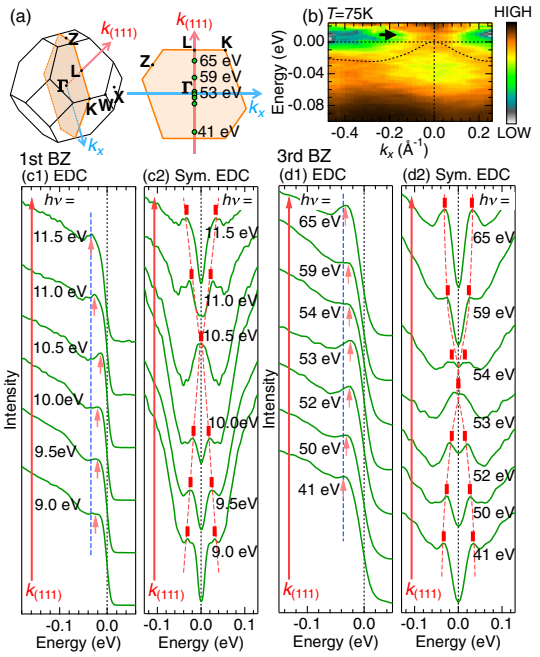

FIG. 2. (a) Brillouin zone for $Nd_2Ir_2O_7$. (b) Band dispersion map crossing Γ, divided by the Fermi function at the measured temperature ($T = 75$ K). The arrow indicates the intensities implying an expected conduction band. EDCs ($T = 15$ K) at $(k_x, k_y) = (0, 0)$ measured with low-energy photons (c1) and high-energy photons (d1), corresponding to $k_{(111)}$s in the first and third Brillouin zone, respectively. (c2), (d2) The same data as in (c1) and (d1), respectively, but symmetrized about E_F. Arrows and bars mark peaks in the spectra.

occurs in $Nd_2Ir_2O_7$ at the same photon energy as in $Pr_2Ir_2O_7$ [22]. To validate this further, we also used higher photon energies reaching the third Brillouin zone [green circles in Fig. 2(a)], and reproduced the Fermi node again at Γ ($h\nu = 53$ eV) as shown in Figs. 2(d1) and 2(d2) [45].

While ARPES is a technique for observing the occupied band structure, one can visualize the unoccupied states slightly above E_F by raising the sample temperature. Figure 2(b) demonstrates such an ARPES image along a k_x cut across Γ. Here, the intensities are divided by the Fermi function at the measured temperature ($T = 75$ K) to properly reveal the spectra above E_F. The spectrum becomes broad due to the short lifetime characteristic of strongly correlated systems at high temperatures, so it is not possible to detect the quasiparticle peaks in the unoccupied side. Nonetheless, significant intensities, indicative of the theoretically predicted conduction band, are visible [a black arrow in Fig. 2(b)].

Intriguingly, the band width of $Nd_2Ir_2O_7$ is found to be extremely narrow, of order ~40 meV on the occupied side, which is much less than expected from density functional theory calculations. While a band narrowing is also reported for the other iridates such as Na_2IrO_3 [32], Sr_2IrO_4 [2], $Sr_3Ir_2O_7$ [33], and $SrIrO_3$ [34], it seems to be comparable or even more significant in the pyrochlore iridates, consistent with dynamical mean-field theory calculations [46]. Furthermore, we detect a peak-dip-hump structure in the spectra, as is often observed in strongly correlated systems. These results are consistent with those of $Pr_2Ir_2O_7$ [22]. The observations in both materials are consistent with a picture of the metallic state as a highly renormalized Fermi liquid [47].

We now turn to the MI transition. In Fig. 3, we examine the temperature evolution of band dispersion through T_{MI}, measured along a momentum cut across Γ [a light blue arrow in the inset of Fig. 3(c)]. Figures 3(a1) and 3(a2) plot the dispersion maps for MI36K symmetrized about E_F and the second derivative of those [45]. Notably, the spectra above and at $T_{MI} \sim 36$ K are virtually identical, showing that there is no significant precursor of the MI transition. As temperature is dropped below T_{MI}, a gap opens at the Fermi node. This variation is also seen in the ARPES mapping at E_F along a k_x–k_y sheet [red plane in the inset of Fig. 3(c)]; the strong intensity at Γ coming from the Fermi node [Fig. 3(d1), $T = 50$ K] vanishes below T_{MI} [Fig. 3(d2), $T = 11$ K]. The band dispersion, determined from the peak or shoulder of the EDC [Fig. 3(c)] also reflects the continuous opening of a gap below T_{MI}. These observations are consistent with a mean-field quasiparticle dispersion, in which the gap is directly controlled by the antiferromagnetic order parameter.

However, the EDCs, themselves, reflect strong correlations. In Figs. 3(b1) and 3(b2), the spectra for $T = 47$ K and 1 K, corresponding to the images in Fig. 3(a1), are plotted. The electronic structure in the metallic phase

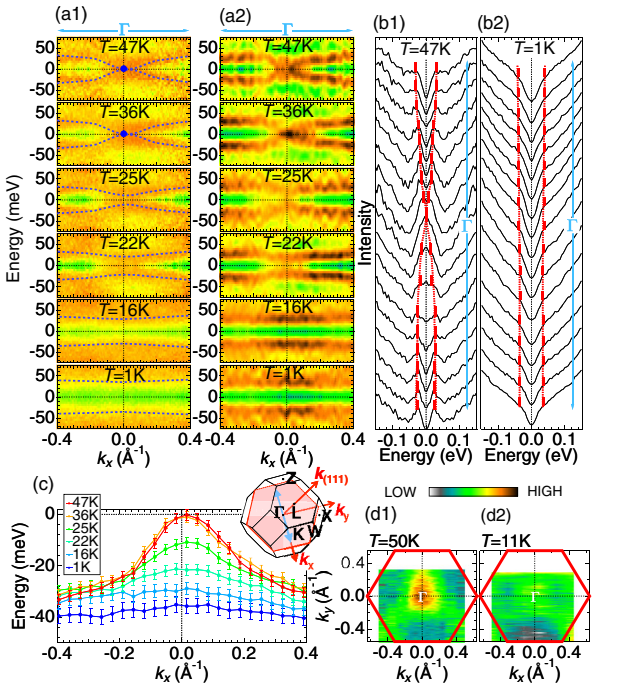

FIG. 3. (a1) Band dispersion map across Γ [$h\nu = 53$ eV; a light blue arrow in the inset of (c)] measured at various temperatures for MI36K. The images are symmetrized about E_F. Blue dashed curves indicate the obtained band dispersions. (a2) Second derivative plots for EDCs in (a1). (b1), (b2) Spectra extracted from (a1) for the metallic phase ($T = 47$ K) and the insulating phase ($T = 1$ K), respectively. (c) Temperature dependence of the band dispersion determined from the spectral peaks or shoulders [red bars in (b1) and (b2)]. (d1), (d2) Spectral intensities at E_F along a momentum sheet crossing Γ [red region in the inset of (c)], measured for the metallic phase ($T = 50$ K) and the insulating phase ($T = 11$ K), respectively.

[Fig. 3(b1)] consists of well-defined quasiparticle peaks (red bars). In contrast, the insulating phase [Fig. 3(b2)] shows a nondispersive flat band, and only the broad spectra lacking long-lived electrons are detected, pointing to correlation-induced Mott localization.

We investigate this further through the detailed variation of spectral-shape at Γ. Figures 4(a1)–4(c1) show the symmetrized EDCs from above to below T_{MI} for the three samples (MI19K, MI25K, and MI36K); the gap is reflected in two split peaks (black arrows) below T_{MI}. Please note that the tracing of peak positions slightly underestimates the "real" onset temperature of gap opening, especially in 3D materials with broadened spectra due to the imperfect sample surface and k_z broadening of ARPES. Nevertheless, the persistence of quasiparticle peaks below but near T_{MI} and their shift with temperature is in accord with a mean-field theory, and denote this as a "Slater picture" [48], though in $Nd_2Ir_2O_7$ there is no unit cell enlargement, as envisioned in the original work of Slater [48], and observed in $NaOsO_3$ [49]. Enlargement is not necessary in $Nd_2Ir_2O_7$ since the unit cell already contains four Ir atoms in the

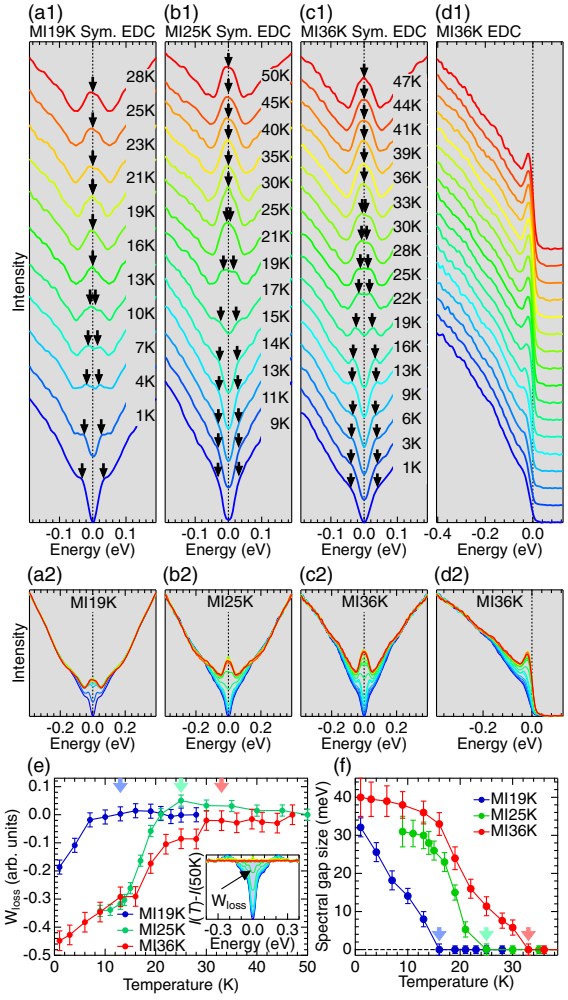

FIG. 4. (a1)–(c1) Temperature evolution of symmetrized EDCs for three samples (MI19K, MI25K, and MI36K) measured at the Γ point. (d1) The same data as in (c1), plotted without symmetrization. (a2)–(d2) The same data as in (a1)–(c1), but without an offset. (e) Temperature dependence of spectral weight loss near E_F (W_{loss}), which is determined to be a negative area in the difference spectra as demonstrated in the inset. (f) Temperature dependence of the magnitude of energy gap estimated from the spectral peak positions marked in (a1)–(c1) by arrows.

metallic state. Our use of the term "Slater" reflects the more fundamental idea that the insulating behavior arises in a mean-field-like way from an exchange field in magnetic order, and follows other usage in the literature [50]. This physics is fully consistent with the observation of coherent muon spin precession, a signature of a long-range magnetic order, just below T_{MI} [24], and the recent discovery of an insulator to metal transition driven by an external magnetic field in $Nd_2Ir_2O_7$ [29,44], revealing that the destruction of AIAO magnetic order restores the metallic transport. The gap behavior we observe here is distinctly different from that in the planar iridate Na_2IrO_3, which remains unchanged across the magnetic transition temperature, and is, thus, categorized as a Mott-type insulator [32].

However, the data show that the quasiparticle peak is significantly suppressed as temperature is further decreased, and it totally disappears at the lowest temperature, leaving only a broad spectrum. The abnormal variation of the quasiparticle peak is also visible in the raw EDCs [Fig. 4(d1)]. While a tiny peak survives in MI19K [see Fig. 4(a1)], even at $T = 1$ K, it is attributable to small carrier doping in the insulating ground state due to the off stoichiometry in the crystal [51]. This is compatible with the previous reports that the electronic state becomes less insulating with an increased off stoichiometry [43,52], eventually turning metallic down to the lowest temperature [53].

The peak suppression is examined in Figs. 4(a2)–4(d2) in more detail, where the spectra of Figs. 4(a1)–4(d1) normalized to the intensities around -0.3 eV are overlapped with each other. The spectral weight at E_F is gradually depleted on cooling down to the lowest temperature. This feature is more clearly demonstrated in Fig. 4(e) by plotting a spectral loss near E_F [W_{loss}, see the inset of Fig. 4(e)] associated with the gap formation. The pseudogaplike spectral loss quantifies the crossover from the Slater-like mean field behavior near T_{MI} to the Mott regime at the lowest temperature. The fact that the gap [Fig. 4(f)] reaches ~30–40 meV at low temperature (comparable to the optical results [31]), thus, is as large as the measured bandwidth, indicates the strong coupling limit, and may be responsible for this crossover. We speculate that the enhancement of exchange field due to Nd ordering at below ~15 K [23] may trigger the increased electron localization observed in ARPES.

Theory predicts that the Weyl points may migrate from the Γ point to the zone boundary and annihilate when the order parameter becomes too large [6,18,21], which may explain their absence in low temperature $Nd_2Ir_2O_7$. One might, therefore, contemplate their reappearance at intermediate temperatures just below T_{MI}, where the gap is smaller and quasiparticles are still well defined. However, no indication of Weyl points at intermediate temperatures was found in the present ARPES measurements. Apart from the difficulty of locating incommensurate temperature-dependent features in ARPES, the progressive destruction of quasiparticles we observed may be another reason for this. We leave a dedicated search for Weyl points just below T_{MI}, perhaps using spin-resolved ARPES, for future work.

In conclusion, we carried out the first ARPES investigation of the MI transition of a three dimensional iridate. We observe a quadratic Fermi node in the metallic state of $Nd_2Ir_2O_7$ very similar to that of $Pr_2Ir_2O_7$. Upon lowering temperature below $T_{\mathrm{MI}} \sim 30$ K, we found a drastic variation in the spectral shape, with a gradual opening of a gap and accompanying suppression of the quasiparticle peak. At the lowest achievable temperature of 1 K, quasiparticles are completely suppressed and a dispersionless spectral edge is observed. The results indicate a crossover from a

Slater-like mean-field effective band insulator just below T_{MI} to a Mott-like insulator with localized electrons at the lowest temperature.

We thank H. Shinaoka and E.-G. Moon for fruitful discussions and constructive comments, and D. Evtushinsky and E. Rienks for technical supports at 1^3 beam line in BESSY-II. We thank H. Z. B. for the allocation of synchrotron radiation beam time. This work was supported by MEXT of Japan (Innovative Area "Topological Materials Science," Grant No. 16H00979), JSPS KAKENHI (Grants No. 25220707, No. 25707030, No. 16H02209, No. 16K13829, and No. 16H06013), the Photon and Quantum Basic Research Coordinated Development Program from MEXT, CREST, JST, Grants-in-Aid for Scientific Research on Innovative Areas (Grants No. 15H05882 and No. 15H05883), and the Program for Advancing Strategic International Networks to Accelerate the Circulation of Talented Researchers (Grant No. R2604) from JSPS. L. B. is supported by DOE Grant No. DE-FG02-08ER46524.

M. N. and T. K. contributed equally to this work.

*kondo1215@issp.u-tokyo.ac.jp

[1] B. J. Kim, H. Ohsumi, T. Komesu, S. Sakai, T. Morita, H. Takagi, and T. Arima, Science **323**, 1329 (2009).
[2] B. J. Kim *et al.*, Phys. Rev. Lett. **101**, 076402 (2008).
[3] J. Kim *et al.*, Nat. Commun. **5**, 4453 (2014).
[4] D. Pesin and L. Balents, Nat. Phys. **6**, 376 (2010).
[5] B.-J. Yang and Y. B. Kim, Phys. Rev. B **82**, 085111 (2010).
[6] W. Witczak-Krempa and Y. B. Kim, Phys. Rev. B **85**, 045124 (2012).
[7] X. Wan, A. M. Turner, A. Vishwanath, and S. Y. Savrasov, Phys. Rev. B **83**, 205101 (2011).
[8] S. Nakatsuji, Y. Machida, J. J. Ishikawa, S. Onoda, Y. Karaki, T. Tayama, and T. Sakakibara, J. Phys. Conf. Ser. **320**, 012056 (2011).
[9] G. Jackeli and G. Khaliullin, Phys. Rev. Lett. **102**, 017205 (2009).
[10] J. Chaloupka, G. Jackeli, and G. Khaliullin, Phys. Rev. Lett. **105**, 027204 (2010).
[11] Y.-Z. You, I. Kimchi, and A. Vishwanath, Phys. Rev. B **86**, 085145 (2012).
[12] S. Nakatsuji, Y. Machida, Y. Maeno, T. Tayama, T. Sakakibara, J. van Duijn, L. Balicas, J. N. Millican, R. T. Macaluso, and Julia Y. Chan, Phys. Rev. Lett. **96**, 087204 (2006).
[13] Y. Tokiwa, J. J. Ishikawa, S. Nakatsuji, and P. Gegenwart, Nat. Mater. **13**, 356 (2014).
[14] D. E. MacLaughlin *et al.*, J. Phys: Conf. Ser. **225**, 012031 (2010).
[15] Y. Machida, S. Nakatsuji, S. Onoda, T. Tayama, and T. Sakakibara, Nature (London) **463**, 210 (2010).
[16] L. Balicas, S. Nakatsuji, Y. Machida, and S. Onoda, Phys. Rev. Lett. **106**, 217204 (2011).
[17] B.-J. Yang and N. Nagaosa, Phys. Rev. Lett. **112**, 246402 (2014).
[18] W. Witczak-Krempa, G. Chen, Y. B. Kim, and L. Balents, Annu. Rev. Condens. Matter Phys. **5**, 57 (2014).
[19] G. Chen and M. Hermele, Phys. Rev. B **86**, 235129 (2012).
[20] L. Savary, E.-G. Moon, and L. Balents, Phys. Rev. X **4**, 041027 (2014).
[21] E.-G. Moon, C. Xu, Y. B. Kim, and L. Balents, Phys. Rev. Lett. **111**, 206401 (2013).
[22] T. Kondo *et al.*, Nat. Commun. **6**, 10042 (2015).
[23] K. Tomiyasu, K. Matsuhira, K. Iwasa, M. Watahiki, S. Takagi, M. Wakeshima, Y. Hinatsu, M. Yokoyama, K. Ohoyama, and K. Yamada, J. Phys. Soc. Jpn. **81**, 034709 (2012).
[24] H. Guo, K. Matsuhira, I. Kawasaki, M. Wakeshima, Y. Hinatsu, I. Watanabe, and Z. A. Xu, Phys. Rev. B **88**, 060411 (2013).
[25] H. Sagayama, D. Uematsu, T. Arima, K. Sugimoto, J. J. Ishikawa, E. O'Farrell, and S. Nakatsuji, Phys. Rev. B **87**, 100403 (2013).
[26] E. Y. Ma, Y.-T. Cui, K. Ueda, S. Tang, K. Chen, N. Tamura, P. M. Wu, J. Fujioka, Y. Tokura, and Z.-X. Shen, Science **350**, 538 (2015).
[27] T.-h. Arima, J. Phys. Soc. Jpn. **82**, 013705 (2013).
[28] Y. Yamaji and M. Imada, Phys. Rev. X **4**, 021035 (2014).
[29] Z. Tian, Y. Kohama, T. Tomita, H. Ishizuka, T. H. Hsieh, J. J. Ishikawa, K. Kindo, L. Balents, and S. Nakatsuji, Nat. Phys. **12**, 134 (2016).
[30] K. Ueda, J. Fujioka, B. J. Yang, J. Shiogai, A. Tsukazaki, S. Nakamura, S. Awaji, N. Nagaosa, and Y. Tokura, Phys. Rev. Lett. **115**, 056402 (2015).
[31] K. Ueda, J. Fujioka, Y. Takahashi, T. Suzuki, S. Ishiwata, T. Taguchi, and Y. Tokura, Phys. Rev. Lett. **109**, 136402 (2012).
[32] R. Comin *et al.*, Phys. Rev. Lett. **109**, 266406 (2012).
[33] P. D. C. King *et al.*, Phys. Rev. B **87**, 241106 (2013).
[34] Y. F. Nie *et al.*, Phys. Rev. Lett. **114**, 016401 (2015).
[35] W. Lotko, R. H. Smith, B. Zhang, J. E. Ouellette, O. J. Brambles, and J. G. Lyon, Science **345**, 184 (2014).
[36] Y. K. Kim, N. H. Sung, J. D. Denlinger, and B. Kim, Nat. Phys. **12**, 37 (2016).
[37] A. de la Torre *et al.*, Phys. Rev. Lett. **115**, 176402 (2015).
[38] A. de la Torre, E. C. Hunter, A. Subedi, S. McKeowh Walker, A. Tamai, T. K. Kim, M. Hoesch, R. S. Perry, A. Georges, and F. Baumberger, Phys. Rev. Lett. **113**, 256402 (2014).
[39] S.-I. Kimura *et al.*, Rev. Sci. Instrum. **81**, 053104 (2010).
[40] K. Matsuhira, M. Wakeshima, Y. Hinatsu, and S. Takagi, J. Phys. Soc. Jpn. **80**, 094701 (2011).
[41] K. Ueda, J. Fujioka, C. Terakura, and Y. Tokura, Phys. Rev. B **92**, 121110 (2015).
[42] M. Sakata, T. Kagayama, K. Shimizu, K. Matsuhira, S. Takagi, M. Wakeshima, and Y. Hinatsu, Phys. Rev. B **83**, 041102 (2011).
[43] J. J. Ishikawa, E. C. T. O'Farrell, and S. Nakatsuji, Phys. Rev. B **85**, 245109 (2012).
[44] K. Ueda, J. Fujioka, B.-J. Yang, J. Shiogai, A. Tsukazaki, S. Nakamura, S. Awaji, N. Nagaosa, and Y. Tokura, Phys. Rev. Lett. **115**, 056402 (2015).
[45] See Supplemental Material at http://link.aps.org/supplemental/10.1103/PhysRevLett.117.056403 for details

about the identification of the Fermi node and additional data for the metal-insulator transition.
[46] H. Shinaoka, S. Hoshino, M. Troyer, and P. Werner, Phys. Rev. Lett. **115**, 156401 (2015).
[47] A "weak" non-Fermi liquid which still possesses quasiparticle peaks would also be compatible [21].
[48] J. C. Slater, Phys. Rev. **82**, 538 (1951).
[49] S. Calder *et al.*, Phys. Rev. Lett. **108**, 257209 (2012).
[50] R. Arita, J. Kuneš, A. V. Kozhevnikov, A. G. Eguiluz, and M. Imada, Phys. Rev. Lett. **108**, 086403 (2012).
[51] Y. Okada *et al.*, Nat. Mater. **12**, 707 (2013).
[52] S. M. Disseler, C. Dhital, T. C. Hogan, A. Amato, S. R. Giblin, C. de la Cruz, A. Daoud-Aladine, S. D. Wilson, and M. J. Graf, Phys. Rev. B **85**, 174441 (2012).
[53] D. Yanagishima and Y. Maeno, J. Phys. Soc. Jpn. **70**, 2880 (2001).